Surface composition and structure of GaN epilayers on sapphire

J. Ahn, M. M. Sung, J. W. Rabalais, D. D. Koleske, and A. E. Wickenden

Citation: The Journal of Chemical Physics **107**, 9577 (1997); doi: 10.1063/1.475255
View online: http://dx.doi.org/10.1063/1.475255
View Table of Contents: http://scitation.aip.org/content/aip/journal/jcp/107/22?ver=pdfcov
Published by the AIP Publishing

Surface composition and structure of GaN epilayers on sapphire

J. Ahn, M. M. Sung, and J. W. Rabalais[a)]
Department of Chemistry, University of Houston, Houston, Texas 77204-5641

D. D. Koleske and A. E. Wickenden
Naval Research Laboratory, Washington, District of Columbia 20375-5347

(Received 23 July 1997; accepted 8 September 1997)

The surface composition and structure of GaN films grown on sapphire substrates by organometallic vapor-phase epitaxy (OMVPE) have been determined through the use of time-of-flight scattering and recoiling spectrometry (TOF-SARS), classical ion trajectory simulations, and low-energy electron diffraction (LEED). TOF-SARS spectra of scattered and recoiled ions plus fast neutrals were collected using 4 keV Ar^+ primary ions. The scattering results were simulated by means of the three-dimensional scattering and recoiling imaging code (SARIC). This data leads to the conclusions that both N-terminated {001}-(1×1) and Ga-terminated {0001}-(1×1) surfaces occur, however no evidence was obtained for mixed terminations. No relaxation or reconstruction was detected on either surface, although both surfaces exhibited two structural domains. The {0001} surfaces are well-ordered and contained hydrogen atoms bound to the N atoms of the outermost layer. The {0001} surfaces are highly reactive towards adsorption of carbon and oxygen from residual gases, however unlike the {0001} surfaces, they adsorb very little hydrogen. These Ga-terminated surfaces are stabilized and obtain more ordered structures as a result of the contamination. © *1997 American Institute of Physics.* [S0021-9606(97)02446-X]

I. INTRODUCTION

GaN and related alloys possess the properties necessary for fabrication of light-emitting diodes and injection diode lasers which operate in the short wavelength region of the visible spectrum. Such applications have resulted in considerable current interest[1–15] in the mechanism of growth of well-ordered GaN films. Growth of GaN epilayers on sapphire by metalorganic chemical vapor deposition (MOCVD) has produced successful devices. The films are typically grown in the direction normal to the {0001} basal plane. This basal plane is similar to the {111} planes of zinc-blende structures. These planes have a polar configuration, i.e., they can be terminated in either of the two atomic subplanes. For GaN, the basal plane can be terminated in either the Ga or N subplanes, i.e., either Ga or N can occupy the first-atomic layer. The polarity of these surfaces can have important effects in semiconductor interfaces. For example, it is known[16] that growth along the Ga- or As-terminated {111} surfaces occurs at different rates and produces surfaces with different degrees of roughness.

It is currently not known whether all GaN heteroepitaxial epilayers have the same elemental termination, different terminations, or mixed terminations. It is important to know these elemental terminations for reproducible growth of GaN films and the subsequent fabrication of devices. Although GaN films have been studied by a host of surface analysis techniques, including low energy electron diffraction (LEED),[17,18] x-ray and ultraviolet photoelectron spectroscopy (XPS and UPS),[17–23] reflection high-energy electron diffraction (RHEED),[24] Auger electron spectroscopy (AES),[17,18] and electron energy loss spectroscopy (EELS),[17,18] the behavior of the surface termination layer is still not understood. Theoretical calculations have predicted that the GaN surface should be unreconstructed[15] and that polarity matching at the film substrate interface is important in determining the surface termination.[25] We have recently[26] studied a GaN film grown on sapphire by MOCVD which exhibited a N-terminated {0001}-(1×1) surface. Using the techniques of time-of-flight scattering and recoiling spectrometry (TOF-SARS), low-energy electron diffraction (LEED), thermal decomposition mass spectrometry (MS), and classical ion trajectory simulations, it was possible to determine that the surface was neither reconstructed nor relaxed, that it was terminated in a N layer, that Ga atoms comprised the second layer, that there were two domains rotated by 60° from each other, and that there were steps on the surface. This particular surface exhibited only N-termination with no evidence for Ga-termination or mixed terminations. We have recently studied several other GaN films grown on sapphire and have found that the films can have either the N- or Ga-terminations. It has also recently been shown[27] using convergent beam electron diffraction that GaN films grown by MOCVD on sapphire have {0001} Ga-terminated surfaces.

In this paper we report on the results of application of the techniques of TOF-SARS, LEED, MS, and simulations to GaN films grown on sapphire substrates by the MOCVD technique. Questions probed were as follows. What is the nature of the terminating element of the films, the crystallographic direction of the heteroepitaxial growth, the reactivity of the films to adsorption of residual gases, to what extent do the surfaces reconstruct or relax, and if so what are the possible surface structures. The results show that both the N- and Ga-terminations can occur on different films and that

a)Author to whom correspondence should be addressed.

these two different surfaces have very different reactivities to residual gases in the vacuum chamber. The high sensitivity of TOF-SARS to surface hydrogen allows one to probe the involvement of hydrogen in the surface structures.

II. EXPERIMENT

A. Analysis techniques

The time-of-flight scattering and recoiling spectrometry (TOF-SARS) technique was used for surface elemental analysis and atomic structure characterization. Details of the TOF-SARS technique have been described elsewhere.[28,29] Briefly, a pulsed noble gas ion beam irradiates the sample surface in a UHV chamber and the scattered and recoiled ions plus fast neutrals are measured by TOF techniques. The primary 4 keV beam employed herein was Ne^+ for scattering from Ga atoms and Ar^+ for recoiling of H, N, and Ga atoms. The ion pulse width was ~ 50 ns, the pulse repetition rate was 30 kHz, and average beam current was 0.5 nA/cm^2. The angular notation is defined as follows: α = beam incident angle to the surface, δ = crystal azimuthal angle, θ = scattering angle, ϕ = recoiling angle, and β = scattering or recoiling exit angle from the surface. Low-energy electron diffraction (LEED) patterns were obtained with Princeton Research Instruments, Inc. reverse view optics.

Classical ion trajectory simulations were carried out by means of the three-dimensional scattering and recoiling imaging code (SARIC) developed in this laboratory.[30] SARIC is based on the binary collision approximation,[31] uses the Zeigler, Biersack, Littmark (ZBL) universal potential[32] to describe the interactions between atoms, and includes both out-of-plane and multiple scattering. Details of the simulation have been published elsewhere.[33]

B. GaN film growth on sapphire

GaN was grown on the *a*-plane $\{11\bar{2}0\}$ of polished sapphire using the Naval Research Laboratory (NRL) facilities. This consisted of a vertical, inductively heated, water-cooled quartz OMVPE reactor at reduced pressure (57 Torr) using H_2 as the carrier gas.[34] After annealing in H_2, the wafer was cooled to ~ 450 °C and a 200 Å nucleation layer of AlN was grown using 1.5 mmole/min triethylaluminum and a 2.5 standard liters/min (slm) flow of NH_3. The substrate was then heated to the growth temperature of 1040 °C and GaN was grown using 53 mmole/min of trimethylgallium under an NH_3 flow of 2.25 slm. The films were uniformly doped using Si_2H_6 at a flow rate of 0.22 standard cubic centimeters/min (sccm).[35] After growth of a 2.7 μm thick GaN film, the substrate was cooled in the NH_3 flow at a rate of 50 °C per minute. The *n*-type films investigated in this study had an electron concentration of 1.2×10^{17} cm^{-3} and a mobility of 325 cm^2/V/s.

C. Cleaning GaN in vacuum

The $\sim 1\times1$ cm^2 samples were cleaned in the UHV chamber (base pressure $<5\times10^{-10}$) used for TOF-SARS at the University of Houston. The samples were mounted on the TOF-SARS sample holder with the sapphire substrate in contact with a Ta plate and held together by small Ta strips over the sample edges. Annealing was achieved by radiative heating and electron bombardment from a tungsten filament mounted behind the Ta plate. Temperatures were measured by means of a pyrometer and a thermocouple which was attached to the sample; the pyrometer readings were calibrated by the thermocouple. The absolute temperature measurements have a maximum uncertainty of ± 20 °C. The clean surface was prepared by cycles of sputtering (1 keV N_2^+ ions, 0.5 μA/cm^2, 10 min) and annealing (10 min) using a dynamic N_2 backfill.

III. RESULTS

The TOF-SARS and LEED measurements were carried out on several different GaN samples which were all grown and cleaned as described above. Since the nature of the surface terminations of the individual samples was not known before the measurements, the several samples investigated provided a random sampling of the terminations. Schematic drawings of the unreconstructed GaN {0001} N-terminated and {0001} Ga-terminated surfaces are shown in Fig. 1; the $\langle 1000\rangle$ azimuth is defined as $\delta = 0°$.

A. LEED results

As will be shown later by TOF-SARS, the samples showed either the {0001} or the {0001} surface terminations. No evidence was found for surfaces with mixed terminations. For the GaN {0001} N-terminated film, a faint (1×1) LEED pattern became discernible at ~ 815 °C and evolved into a sharp hexagonal (1×1) pattern at ~ 920 °C. Upon continued heating to 1000 °C, a diffuse background and satellite spots around the hexagonal spots were observed, indicating possible surface faceting. Hydrogen was always present on the surface (as will be shown by TOF-SARS) when the sharp (1×1) pattern was observed. For the GaN {0001} Ga-terminated film, a very diffuse (1×1) pattern appeared at ~ 920 °C and became worse after heating to 1000 °C. The clean GaN {0001} surface with the diffuse (1×1) LEED pattern evolved into a sharp hexagonal (1×1) pattern after exposing the surface for 1 h under vacuum at room temperature. The hydrogen concentration of the clean {0001} surface was always much lower than that of the {0001} surface.

B. Termination layer

Elemental analysis was obtained by matching the observed TOF peaks to those predicted by the binary collision approximation.[31] The first-layer elemental species was determined by using grazing incidence ($\alpha = 6°$) TOF-SARS at random azimuthal angles and a scattering-recoiling angle of $\theta = \phi = 40°$. Using random azimuthal angles and a low incident angle avoids the anisotropic effects of scattering along the principal low-index azimuths and provides scattering intensities which are from the first-atomic layer and exposed atoms in the second-atomic layer.

Typical TOF spectra from both clean GaN $\{000\bar{1}\}$ and {0001} surfaces taken along a random azimuthal direction

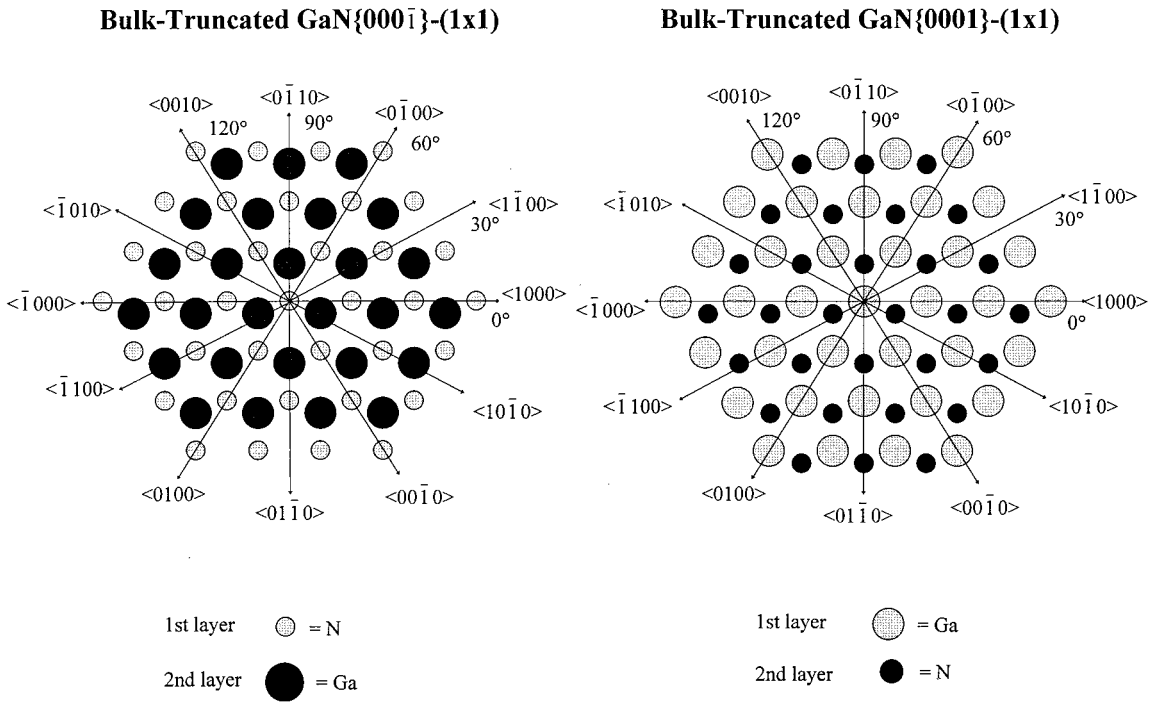

FIG. 1. Plan view of the ideal bulk-terminated GaN{000$\bar{1}$}-(1×1) N-terminated and {0001}-(1×1) Ga-terminated surfaces illustrating the azimuthal angle δ assignments. Another domain is obtained by 60° rotation of this surface about the surface normal.

(not aligned along a high symmetry azimuth) with a grazing incident angle α are shown in Fig. 2. The spectra exhibit peaks due to scattering of Ar from Ga atoms and recoiling of H, N, and Ga atoms. The scattering angle used ($\theta=40°$) is above the critical angle for Ar single scattering from N atoms ($\theta_c=20.5°$); this results in a negligible contribution of the N atoms to the scattering peak intensity. The relative elemental concentrations in the surface layers were obtained from spectra which were collected at five different random azimuthal angles. The relative H, N, and Ga recoil intensities were obtained from the average of these five spectra, from which concentrations were calculated after background subtraction and correction for the different recoiling cross sections. The cross sections were calculated[36] in the binary collision approximation using the Moliere approximation to the potential function. These calculated cross sections and relative atomic concentrations are listed in Table I. The Ga scattering peak and H and N recoiling peaks were used for the concentration determinations. Relative concentrations obtained in this manner have an uncertainty on the order of 30%, primarily due to shadowing and blocking effects which are not corrected along the random azimuths.

The sample with the high ratio of [Ga]/[N]=1.82 in Table I indicates that this particular surface is terminated in a layer of Ga atoms; it will henceforth be identified as the GaN {0001} Ga-terminated surface. The sample with the low ratio of [Ga]/[N]=0.52 in Table I indicates that this particular surface is terminated in a layer of N atoms; it will henceforth be identified as the GaN {0001} N-terminated surface. The Ga-terminated surface exhibits a very low H recoil intensity after cleaning, whereas the N-terminated surface exhibits a high recoil H intensity. The intense H recoil peak on the N-terminated surface was present under all conditions that gave rise to the clear (1×1) LEED pattern, indicating that the H concentration on the (1×1) surface is comparable to the N concentration.

The Ga-terminated GaN{0001}-(1×1) surface was very

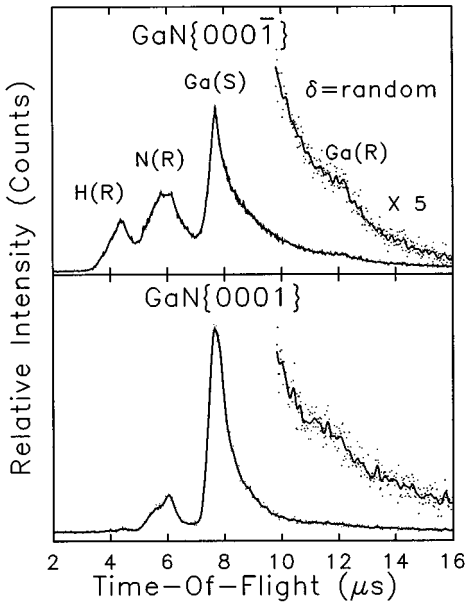

FIG. 2. TOF-SARS spectra of 4 keV Ar^+ scattering from GaN{000$\bar{1}$} and {0001} surfaces with the ion beam aligned along a random azimuthal direction. Incident angle $\alpha=6°$; Scattering angle $\theta=40°$.

TABLE I. Calculated cross sections (σ) for 4 keV Ar^+ scattering from Ga atoms and recoiling of H, N, and Ga atoms, relative atomic concentrations from experimental intensities along random azimuths, and ASEA values.

Scattering (S) and Recoiling (R) Cross sections (σ) [Å^2]			
$\sigma_{Ga}(S)$	$\sigma_H(R)$	$\sigma_N(R)$	$\sigma_{Ga}(R)$
0.21	0.13	0.071	0.099
Relative surface atomic concentrations			
Clean GaN{0001̄} surface	[N]=1	[H]=0.71	[Ga]=0.52
Clean GaN{0001} surface	[N]=1	[H]=0.08	[Ga]=1.82
Experimental[a] ASEA values along the 0° ⟨1000⟩ and 30° ⟨11̄00⟩ azimuths			
GaN{0001̄}-(1×1) surface	$(I_{30°}/I_{0°})_N=1.0$	$(I_{30°}/I_{0°})_H=1.1$	$(I_{30°}/I_{0°})_{Ga}=0.59$
GaN{0001}-(1×1) surface	$(I_{30°}/I_{0°})_N=0.92$	$(I_{30°}/I_{0°})_H=0.91$	$(I_{30°}/I_{0°})_{Ga}=2.01$

[a]Ratios of recoiling peaks for N and H and scattering peaks for Ga were used in calculating the ASEA values.

reactive while the N-terminated GaN{0001̄}-(1×1) surface was quite inert towards adsorption of residual gases. This is evidenced by the time evolution of the TOF spectrum as shown in Fig. 3, which was taken along a random azimuth. The *A* spectrum for the GaN{0001}-(1×1) surface was recorded immediately after cleaning and the *B* spectrum was recorded approximately 1 h after cleaning. The relative intensities of the recoiling and scattering peaks in the TOF spectrum of this Ga-terminated surface start changing as a function of time as soon as the cleaning procedure is finished. The intensities of the H and N recoil peaks increase while the intensity of the Ar scattering peak from Ga atoms decreases. The intensity increase at the N recoil position has contributions from C and O atom recoiling; under these resolution conditions, these masses are not resolved from the mass of N. No further change in the TOF spectrum was observed after the sample remained in vacuum for ~12 h (spectrum *C*). It is noteworthy that the H recoil intensity on this {0001} surface is still lower than that from the {0001} surface even hours after cleaning. The extremely diffuse (1×1) LEED pattern of this {0001} surface taken just after cleaning changes into a sharper (1×1) pattern after exposure to residual gases, indicating that a more ordered surface structure is obtained with contamination.

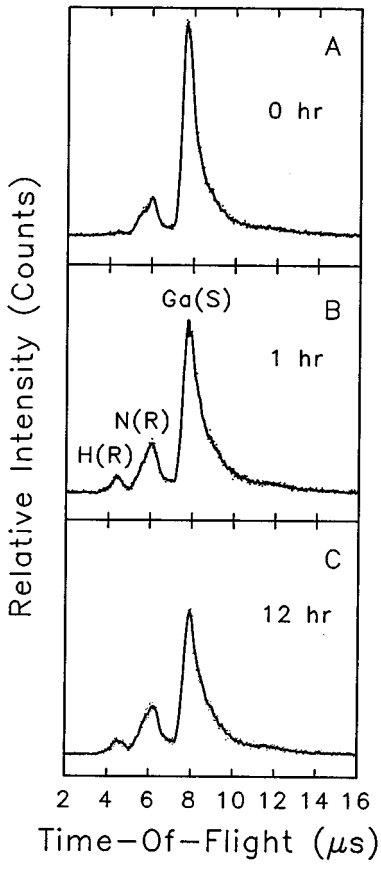

FIG. 3. TOF-SARS spectra of 4 keV Ar^+ scattering from a GaN{0001} surface as a function of time after cleaning the surface. The ion beam is aligned along a random azimuthal direction. Incident angle $\alpha=6°$; Scattering angle $\theta=40°$.

C. Bulk crystallographic directions

The composition from azimuth-specific elemental accessibilities (CASEA) method[37] provides information on the relative elemental accessibilities along selected low index azimuths. These values are useful in confirming the results from the elemental analysis and the compatibility of that analysis with the crystal structure. For CASEA, the scattering or recoiling peak intensities are measured under conditions of low incident angle α, low exit angle β, and alignment of the beam along selected low index azimuths δ. Due to the shadowing and blocking effects, measurements taken under these conditions provide scattering and recoiling intensities which result from only those layers of atoms that are directly exposed to the vacuum. Since only the first- and second-layer atoms or atoms exposed in missing-row troughs, are accessible to the beam under these conditions, azimuth-specific elemental accessibilities (ASEA) along the azimuths are obtained. These ASEA results are used in relating the orientation of the surface symmetry elements, i.e., the features of the LEED pattern, as follows. For a given element (i), the ASEA is the ratio of scattering or recoiling intensities (I) from the element along two different azimuthal directions (χ and δ) of the crystal. Using a simple shadow cone approximation, the ASEA is equal to the ratio

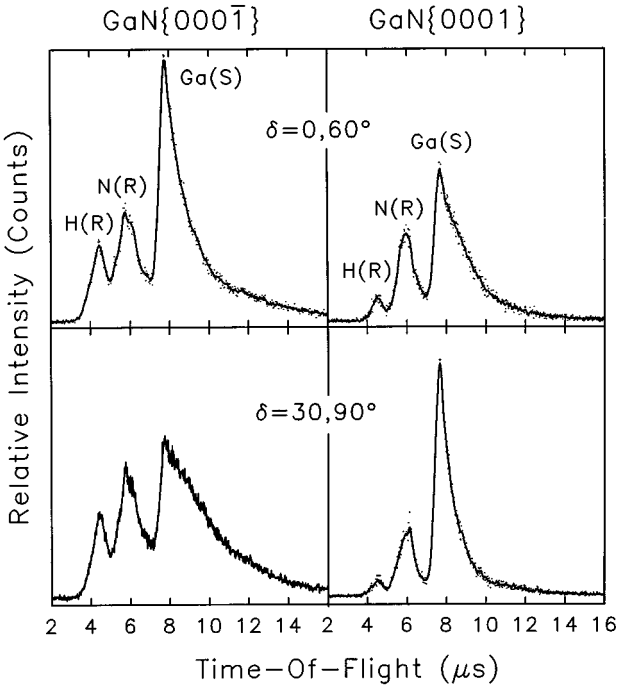

FIG. 4. Typical TOF-SARS spectra of 4 keV Ar^+ scattering from GaN{0001} and {0001} surfaces with the ion beam directed along the ⟨1000⟩ ($\delta=0°$) and ⟨1100⟩ ($\delta=30°$) directions. Spectra from $\delta=60°$ were identical to those from $\delta=0°$ and spectra from $\delta=90°$ were identical to those from $\delta=30°$. Incident angle $\alpha=12°$; Scattering angle $\theta=40°$.

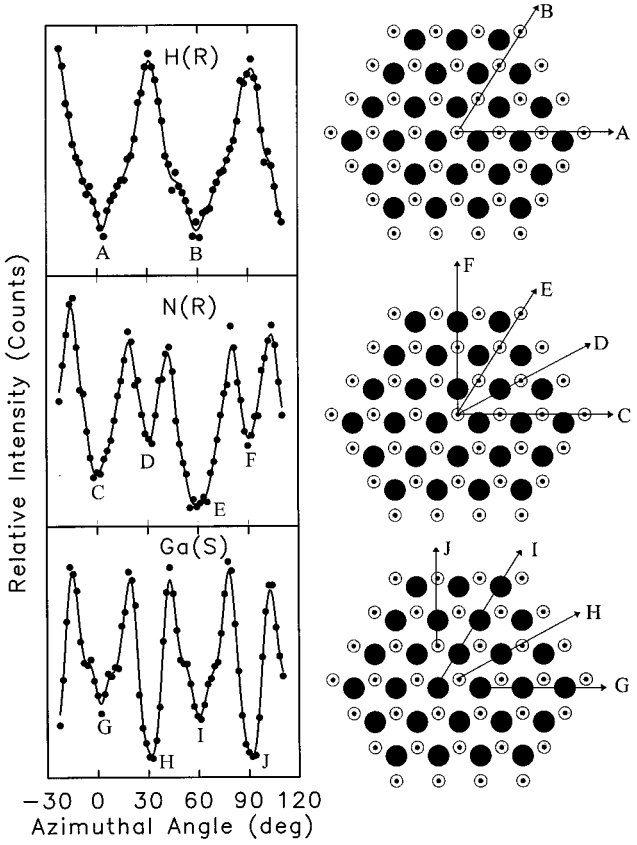

FIG. 5. Azimuthal angle δ-scans of hydrogen atom recoil H(R), nitrogen atom recoil N(R), and Ar^+ scattering from Ga atoms Ga(S) on the GaN{0001} surface. The projectile was 4 keV Ar^+ and the conditions were $\alpha=20°$, $\theta=30°$ for H(R), $\alpha=10°$, $\theta=40°$ for N(R), and $\alpha=12°$, $\theta=90°$ for Ga(S).

of the number of atoms $[N_\delta/N_\lambda]$ exposed to the beam in the surface unit cell of the surface phase for the two azimuths, i.e.

$$(I_x/I_\delta)_i=\mathrm{ASEA}=(N_x/N_\delta)_i\,.$$

This ratio is independent of scattering and recoiling cross section corrections.

It will be sufficient to observe the ASEA values along the 0° and 30° azimuths because there are two domains on the surfaces (as will be shown later). Along the 0° azimuth, the second-layer atoms are partially shadowed by the first-layer atoms because the lateral spacing between them is only 0.9 Å and the radii of the shadow cones are of the order of 1 Å. Along the 30° azimuth, it is possible for the first-layer atoms to totally shadow second-layer atoms, making them inaccessible for scattering. Note that the degree of shadowing is different for projectiles approaching along the 30° or 90° directions due to the arrangement of the first- and second-layer atoms. However, the I_{Ga} and I_N intensity ratios along the 30° and 90° directions are the same for both the {0001} and {0001} surfaces; this indicates that both of the surfaces have two spatial domains which are rotated by 60°. Example spectra used in obtaining the ASEA values are shown in Fig. 4 and the results are listed in Table I.

The Ga scattering intensities will be used for the ASEA values rather than the N recoiling intensities because the N atom ASEA values may be unreliable as a result of possible overlapping of C and O contamination peaks. For the {0001}-(1×1) N-terminated surface, the second-layer Ga accessibility is extremely sensitive to azimuthal direction; specifically, it is greatly reduced along the 30° and 90° directions relative to the 0° and 60° directions. This is due to shadowing and blocking by first-layer N atoms. This confirms that these directions correspond to the ⟨1100⟩ azimuth or similar azimuths which are rotated by 60°, such as ⟨0110⟩, ⟨1010⟩, ⟨1100⟩, ⟨0110⟩, or ⟨1010⟩ (see Fig. 1). For the {0001}-(1×1) Ga-terminated surface, the first-layer Ga accessibility is greatly reduced along the 0° and 60° directions relative to the 30° and 90° directions. This is due to the enhanced self-shadowing and -blocking of Ga atoms by neighboring Ga atoms along the 0° and 60° directions as a result of the short interatomic spacings. Self-shadowing and blocking are reduced along the 30° and 90° azimuths due to the long interatomic spacings. This confirms that the 0° and 60° directions correspond to the ⟨1000⟩ azimuth or similar azimuths which are rotated by 60°, such as ⟨0100⟩, ⟨0010⟩, ⟨1000⟩, ⟨0100⟩, or ⟨0010⟩ (see Fig. 1).

D. Surface periodicities of the H, N, and Ga atoms

The surface periodicities[38,39] of the H, N, and Ga atoms were determined by monitoring I_{Ga} for Ar scattering from Ga atoms and I_H and I_N for Ar recoiling of H and N atoms as a function of crystal azimuthal angle δ. Figures 5 and 6 show

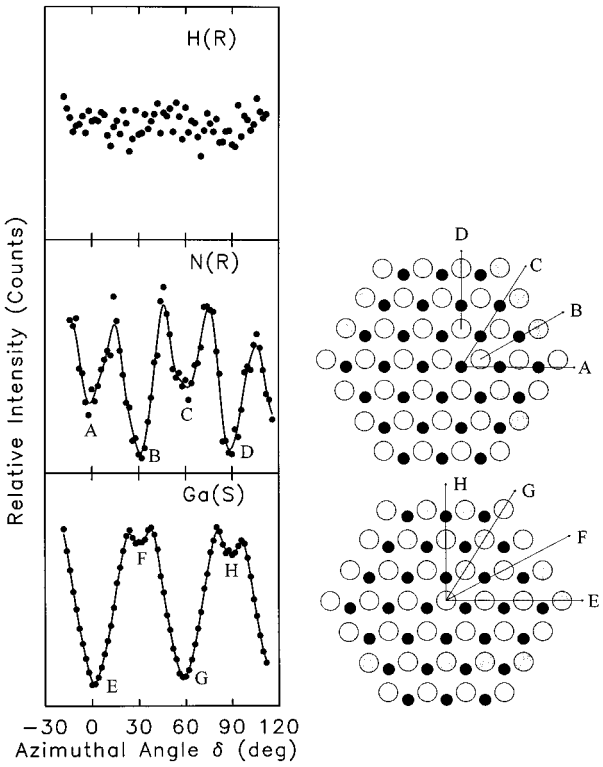

FIG. 6. Azimuthal angle δ-scans of hydrogen atom recoil H(R), nitrogen atom recoil N(R), and Ar^+ scattering from Ga atoms Ga(S) on the GaN{0001} surface. The scattering conditions are identical to those of Fig. 5.

the azimuthal anisotropy of scattering and recoiling intensities for both the {0001} and {0001} surfaces, respectively. The same scattering parameters were used in these δ-scans of both the {0001} and {0001} surfaces. The minima are coincident with low index azimuths where the surface atoms are inside of the shadowing or blocking cones cast by their aligned, closely spaced nearest neighbors, resulting in low intensities. Wide, deep minima are expected from short interatomic spacings because of the larger degree of rotation about δ required for atoms to emerge from neighboring shadows. Schematic diagrams of the surface structures illustrating the scattering and blocking directions are presented along with the δ-scans.

The I_N δ-scans of Figs. 5 and 6 were performed in the shadowing mode, i.e., a grazing incident angle of $\alpha = 10°$ was used. For the {0001} surface (Fig. 5) the data exhibit minima every 30°, with the minima labeled 0° (C) and 60° (E) being deeper than those at 30° (D) and 90° (F). The 0° and 60° directions correspond to the ⟨1000⟩ and ⟨0100⟩ azimuths, respectively, where the N–N interatomic spacings are shortest and self-shadowing of first-layer N atoms by neighboring first-layer N atoms is most efficient. The 30° and 90° minima correspond to the ⟨1100⟩ and ⟨0110⟩ azimuths, respectively, where the N–N interatomic spacings are longer and self-shadowing is less efficient. The {0001} surface (Fig. 6) has a very similar I_N azimuthal pattern, except that there is a 30° shift in the position of each corresponding minimum with respect to that of the $\{000\bar{1}\}$ surface, i.e., the minima along 30° (B) and 90° (D) are deeper than those at 0° (A) and 60° (C). The second-layer N atoms are efficiently shadowed at 30° and 90° by the first-layer Ga atoms, although they are only partially shadowed and blocked at 0° and 60°. As shown in the model (Fig. 1), the degree of shadowing and blocking along the 30° and 90° azimuths is not identical due to the relationship of the first- and second-layer atoms. The minima observed at these two angles have identical widths and depths, suggesting that the surface exists in two different domains, if there would be only one domain, different widths and depths for these minima would be expected.

The I_{Ga} δ-scans of Figs. 5 and 6 were performed under the same experimental conditions as for I_N. For the {0001} surface (Fig. 5), the data also exhibit minima every 30°, but in contrast to the I_N minima, the minima labeled 30° (H) and 90° (J) are much deeper than those at 0° (G) and 60° (I). Shadowing and blocking of second-layer Ga by first-layer N is most efficient along the 30° and 90° directions due to the aligned overlayer N atoms. Along the 0° and 60° directions, the overlayer N atoms are not aligned with Ga atoms, resulting in less severe shadowing and blocking. The minima observed at 30° and 90° have identical widths and depths, also suggesting that the surface exists in two different domains. The periodicity of the I_{Ga} δ-scan of the {0001} surface (Fig. 6) shows a 30° shift, in terms of the positions of minima, with respect to that of {0001} surface. The shallow minima along the 30° (F) and 90° (H) azimuths result from the long interatomic spacings along these directions and the deep minima at 0° (E) and 60° (G) result from the short interatomic spacings along these directions.

The I_H δ-scans of Figs. 5 and 6 were performed in the blocking mode i.e., a small exit angle $\beta = 10°$ was used. For the {0001} surface (Fig. 5), the data exhibit 60° periodicity with deep minima along the 0° and 60° directions, unlike the I_N and I_{Ga} scans. The H atoms are too light to cause significant shadowing of the incoming Ar projectiles. However, recoiled H atoms can be blocked by first-layer neighboring N atoms. The radii of the shadowing and blocking cones for H atom collisions with N and Ga atoms are only ~ 0.3 Å compared to >1 Å for Ne^+ and Ar^+ collisions with N and Ga atoms.[38] By using a small exit angle β, recoiled H atoms can be blocked by nearest-neighbor N atoms. The observed periodicity arises if the H atoms are bound to the outerlayer N atoms and protruding outward from the surface plane. The short H–N interatomic spacings along 0° and 60° result in overlayer recoiled H atoms being blocked by their first-layer N neighbors. Along the 30° and 90° directions, the H–N interatomic spacings are longer and the recoiling H trajectories are outside of the neighboring N atom blocking cones. In contrast to the I_H δ-scan of the {0001} surface, the {0001} surface (Fig. 6) shows no appreciable periodicity in the I_H δ-scan. This indicates the H atoms are most likely randomly distributed on the surface,

Trajectory simulations of the δ-scans were carried out by using two structural domains which were rotated by 60° from each other. Combining two such domains results in symmetrical δ-scans which are good reproductions of the experi-

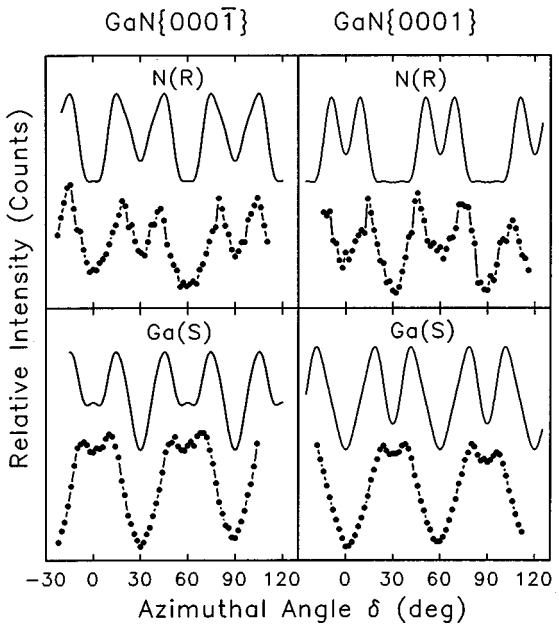

FIG. 7. Trajectory simulations of the azimuthal angle δ-scans of nitrogen atom recoil N(R) and Ar^+ scattering from Ga atoms Ga(S) along the {0001} and {0001} surfaces using the same conditions as listed in Fig. 5. Two different domains were used in the simulations. The black dots are the experimental spectra (from Figs. 5 and 6) and the lines are the simulations.

mental scans as shown in Fig. 7. The simulation results clearly show the 30° shift in the periodicity of the oscillations in I_N and I_{Ga} δ-scans, consistent with the experimental results. The amplitudes of the oscillations in the N(R) simulations are similar to those observed experimentally, however the amplitudes in the Ga(S) simulations are much greater than those observed experimentally. The amplitudes of these shadowing and blocking oscillations are strongly dependent on the screening factors used in the scattering potentials, however the positions of the minima are not influenced by these factors. Rather than choose different screening factors to obtain the best agreement for each individual case, we chose a single screening factor and applied to all cases.

IV. DISCUSSION

Our results show that there are two distinct types of atomic terminations for the GaN samples studied, i.e., N-terminated {0001}-(1×1) and Ga-terminated {0001}-(1×1) surfaces. The nature of the termination layer is expected to depend on polarity matching considerations between the substrate and film. Recent *ab initio* total energy calculations by Capaz *et al.*[25] have shown that the lowest energy interfaces are expected to be those on which cations (anions) of the substrate bind to anions (cations) of the film. Hence, the final polarity of the film is strongly dependent on the polarity of the substrate. Therefore, the nature of the surface termination of the sapphire substrate may be important to understanding the effects of substrate structure on the epitaxial relationship and overlayer lattice structure in thin film deposition. It is interesting that although the films used in our experiment were all grown on {11$\bar{2}$0} (a-plane) sapphire surfaces, our results show that some are N-terminated and others are Ga-terminated. It is possible that the surface structure of the {1120} face of sapphire can be terminated with ether O-rich or Al-rich surface monolayers. The surfaces of our {1120} sapphire substrates have not been studied to determine their terminations. If the layer ordering in GaN films is preserved during their growth, the occurrence of Ga- or N-terminations in the films may depend on different terminations of the sapphire substrates.

The bulk terminated polar surfaces of compound semiconductor surfaces are typically unstable due to the partial electron occupancies of their dangling bonds.[40] These surfaces achieve stability and semiconducting behavior by reconstructing in a manner in which the dangling bonds either coalesce into dimer bonds or become completely filled or empty by electron transfer from the more electropositive to the more electronegative elements. Such a situation results in a semiconducting surface in which all dangling bonds are either completely filled or empty, i.e., the surface is autocompensated.[39,41]

A clean unreconstructed GaN{000$\bar{1}$}-(1×1) surface has first-layer N and second-layer Ga atoms which are sp^3 hybridized. This results in N dangling bonds protruding from the surface which each have 5/4e and, therefore, a deficiency of 3/4e. Autocompensation of this surface can be achieved either by reconstruction or by bonding of these N dangling bonds to foreign atoms which can donate electron density to fulfill the deficiency; H atoms can fulfill this requirement for the {0001} surface. Since the surface is not reconstructed and H coverage of the N atoms was observed by TOF-SARS under all conditions where a sharp (1×1) LEED pattern was observed, we propose that the surface is H stabilized.

In contrast to the stability of the {0001}-(1×1) surface, the clean {0001}-(1×1) surface shows noticeable reactivity. As shown in Fig. 3, the relative concentrations of the elements composing the surface change as a function of time after cleaning until the surface finally reaches equilibrium. An extremely small amount of H is observed shortly after cleaning the surface. The (1×1) LEED pattern from this surface is very diffuse. The increase in the relative intensities of the H, C, and O contaminants with respect to the Ga scattering peak was accompanied by a sharpening of the LEED pattern, indicating an improved surface ordering with more contamination. No further change in the TOF spectrum after approximately 12 h in the vacuum implies that the surface has been stabilized. Note that the H content remains very low compared to that of the N-terminated surface even after 12 h. Since this surface is not reconstructed in spite of the low H concentration, it must be stabilized by other chemical species in order to satisfy the autocompensation requirements. The apparent increase of the N, C, and O recoiling peak (they are not resolved in the TOF spectrum) as the surface ages suggests that the surface is adsorbing contaminant C and O. The sharper (1×1) LEED pattern observed from this contaminated surface suggests that the small amount of contaminant atoms are randomly distributed over the {0001} surface leading to stabilization.

V. CONCLUSIONS

The results obtained from the TOF-SARS, LEED, and trajectory simulation studies of the GaN surfaces can be summarized as follows.

(1) Both N-terminated $\{000\bar{1}\}$-(1×1) and Ga-terminated $\{0001\}$-(1×1) surfaces have been identified for GaN films grown by OMVPE on $\{11\bar{2}0\}$ (a-plane) sapphire surfaces. No evidence of the presence of mixed terminations was observed within the TOF-SARS sensitivity of $\sim10^{13}$ atoms/cm^2.

(ii) For the $\{000\bar{1}\}$ surface, as found in our previous work, hydrogen atoms are bound to the N atoms of the outmost layer with a coverage of $\sim3/4$ of a monolayer and protrude outward from the surface. The $\{000\bar{1}\}$ surface is highly reactive towards adsorption of carbon and oxygen from residual gases (H_2O, CO, hydrocarbons) in the vacuum chamber, however unlike the $\{0001\}$ surface, it adsorbs very little hydrogen. This Ga-terminated surface is stabilized and has a more ordered structure as a result of the contamination.

(iii) Both surfaces are bulk terminated with no detectable reconstruction or relaxation within the accuracy of the TOF-SARS measurements, i.e., ±0.2 Å. LEED indicates that the long-range order is affected by the adsorption of gases. The truly clean surface may undergo some reconstruction or relaxation relative to the bulk.

(iv) Both surfaces exhibit two structural domains.

ACKNOWLEDGMENT

This work was supported primarily by the MRSEC Program of the National Science Foundation under Award Number DMR-9632667.

[1] R. F. Davis, Proc. IEEE **79**, 702 (1991).
[2] S. Strite and H. Morkoc, J. Vac. Sci. Technol. B **10**, 1237 (1992).
[3] S. N. Mohammad, A. A. Salvador, and H. Morkoc, Proc. IEEE **83**, 1306 (1995).
[4] J. E. Jaffe, R. Pandey, and P. Zapol, Phys. Rev. B **53**, 1 (1996).
[5] S. Nakamura, M. Senoh, and T. Mukai, Appl. Phys. Lett. **64**, 1687 (1994).
[6] H. Morkoc and S. N. Mohammad, Science **267**, 51 (1995).
[7] S. Nakamura, M. Senoh, S. Nagahama, N, Iwasa, T. Yamada, T. Matsushita, H, Kiyoku, and Y. Sugimoto, Jpn. J. Appl. Phys. **35**, L74 (1996).
[8] D. K. Gaskill, A. E. Wickenden, K. Doverspike, B. Tadayon, and L. B. Rowland, J. Electron. Mater. **24**, 1525 (1995).
[9] J. Neugebauer and C. G. Van de Walle, Phys. Rev. Lett. **75**, 4452 (1995).
[10] R. G. Wilson, S. J. Pearton, C. R. Abernathy, and J. M. Zavada, J. Vac. Sci. Technol. A **13**, 719 (1995).
[11] S. Nakamura, N. Iwasa, M. Senoh, and T. Mukai, Jpn. J. Appl. Phys. **31**, 1258 (1992).
[12] H. Amano, M. Kito, K. Hiramatsu, and I. Akasaki, Jpn. J. Appl. Phys. **38**, L2112 (1989).
[13] J. Neugebauer and C. G. Van de Walle, Appl. Phys. Lett. **68**, 1829 (1996).
[14] T. Sasaki and T. Matsuoka, J. Appl. Phys. **64**, 4531 (1988).
[15] P. Boguslawski, E. L. Briggs, and J. Bernholc, Phys. Rev. B **51**, 17255 (1995).
[16] R. E. Ewing and P. E. Greene, J. Electrochem. Soc. **11**, 1266 (1964).
[17] V. M. Bermudez, R. Kaplan, M. A. Khan, and J. N. Kuznia, Phys. Rev. B **48**, 2463 (1993).
[18] M. Asif Khan, J. N. Kuznia, D. T. Olson, and R. Kaplan, J. Appl. Phys. **73**, 3108 (1993).
[19] J. Hedman and N. Martensson, Phys. Scr. **22**, 176 (1980).
[20] R. Carin, J. P. Deville, and J. Werckmann, Surf. Interface Anal. **16**, 65 (1990).
[21] D. Troost, H.-U. Baier, A. Berger, and W. Monch, Surf. Sci. **242**, 324 (1991).
[22] L. A. DeLouise, J. Vac. Sci. Technol. A **10**, 1637 (1992).
[23] X.-Y. Zhu, M. Wolf, T. Huett, and J. M. White, J. Chem. Phys. **97**, 5856 (1992).
[24] Z. Yang, L. K. Li, and W. I. Wang, Appl. Phys. Lett. **67**, 1686 (1995); K. Iwata, H. Asahi, S. J. Yu, K. Asami, H. Fujita, M. Fushida, and S. Gonda, Jpn. J. Appl. Phys. **35**, L289 (1996); M. E. Lin, S. Strite, A. Agarwal, A. Salvador, G. L. Zhou, N. Teraguchi, A. Rockett, and H. Morkoc, Appl. Phys. Lett. **62**, 702 (1993); H. Liu, A. C. Frenkel, J. G. Kim, and R. M. Park, J. Appl. Phys. **74**, 6124 (1993); S. Fujita, M. A. L. Johnson, W. H. Rowland, W. C. Hughes, Y. W. He, N. A. Elmasry, J. W. Cook, Jr., J. F. Schetzina, J Ren, and J. A. Edmond, Ext. Abstr. Int. Conf. Sol. St. Devices and Materials, Oxaka, 1995, p. 692.
[25] R. B. Capaz, H. Lim, and J D. Joannopoulos, Phys. Rev. B **51**, 17755 (1995).
[26] M. M. Sung, J. Ahn, V. Bykov, J. W. Rabalais, D. D. Koleske, and A. E. Wickenden, Phys. Rev. B **54**, 14652 (1996).
[27] F. A. Ponce, D. P Bour, W. T. Young, M. Saunders, and J. W. Steeds, Appl. Phys. Lett. **69**, 337 (1996).
[28] J. W. Rabalais, Science **250**, 521 (1990).
[29] O. Grizzi, M. Shi, H. Bu, and J. W. Rabalais, Rev. Sci. Instrum. **61**, 740 (1990)
[30] M. M. Sung, V. Bykov, A. Al-Bayati, C. Kim, S. S. Todorov, and J. W. Rabalais, Scanning Microsc. **9**, 321 (1995).
[31] E. S. Parilis, L. M. Kishinevsky, N. Yu. Turaev, B. E. Baklitzky, F. F Umarov, V Kh Verleger, S. L. Nizhnaya, and I. S. Bitensky, *Atomic Collisions on Solid Surfaces* (North-Holland, New York, 1993).
[32] J. F. Zeigler, J. P. Biersack, and U. Littmark, *The Stopping and Range of Ions in Solids*, edited by J. F. Ziegler (Pergamon, New York, 1985).
[33] V. Bykov, C. Kim, M. M. Sung, K. J. Boyd, S. S. Todorov, and J W Rabalais, Nucl. Instrum. Methods Phys. Res. B **114**, 371 (1996).
[34] L. B. Rowland, K. Doverspike, A. Giordana, M. Fatemi, D. K. Gaskill, M. Skowronski, and J. A. Freitas, Jr. *Silicon Carbide and Related Materials*, edited by M. G. Spencer, R. P. Devaty, J. A. Edmond, M. A. Khan, R. Kaplan, and M. Rahman (Bristol: Inst. Phys., 1994), p. 429.
[35] A. E. Wickenden, L. B. Rowland, K. Doverspike, D. K. Gaskill, J. A. Freitas, Jr., D. S. Simons, and P. H. Chi, J. Electron. Mater. **24**, 1547 (1995).
[36] J. W. Rabalais, CRC Crit. Rev. Solid State Mater. Sci. **14**, 319 (1988).
[37] M. M. Sung, C. Kim, and J. W. Rabalais, Nucl. Instrum. Methods Phys. Res. B **118**, 522 (1995).
[38] O. Grizzi, M. Shi, H. Bu, and J. W. Rabalais, Phys. Rev. B **40**, 10127 (1989).
[39] M. M. Sung, C. Kim, H. Bu, D. S. Karpuzov, and J. W. Rabalais, Surf. Sci. **322**, 116 (1995).
[40] For a recent review see C. B. Duke, Scanning Microsc. **8**, 753 (1994).
[41] M. D. Pashley, Phys. Rev. B **40**, 10481 (1989).